

Alma Mater Studiorum Università di Bologna
Archivio istituzionale della ricerca

Tantalum nanoparticles enhance the osteoinductivity of multiscale composites based on poly(lactide-co-glycolide) electrospun fibers embedded in a gelatin hydrogel

This is the final peer-reviewed author's accepted manuscript (postprint) of the following publication:

Published Version:

A. Liguori, M.E. Gino, S. Panzavolta, P. Torricelli, M. Maglio, A. Parrilli, et al. (2022). Tantalum nanoparticles enhance the osteoinductivity of multiscale composites based on poly(lactide-co-glycolide) electrospun fibers embedded in a gelatin hydrogel. MATERIALS TODAY CHEMISTRY, 24, 1-12 [10.1016/j.mtchem.2022.100804].

Availability:

This version is available at: <https://hdl.handle.net/11585/902305> since: 2022-11-13

Published:

DOI: <http://doi.org/10.1016/j.mtchem.2022.100804>

Terms of use:

Some rights reserved. The terms and conditions for the reuse of this version of the manuscript are specified in the publishing policy. For all terms of use and more information see the publisher's website.

This item was downloaded from IRIS Università di Bologna (<https://cris.unibo.it/>).
When citing, please refer to the published version.

(Article begins on next page)

This is the final peer-reviewed accepted manuscript of:

LIGUORI, A.; GINO, M. E.; PANZAVOLTA, S.; TORRICELLI, P.; MAGLIO, M.; PARRILLI, A.; GUALANDI, C.; GRIFFONI, C.; BARBANTI BRODANO, G.; FINI, M.; FOCARETE, M. L. TANTALUM NANOPARTICLES ENHANCE THE OSTEOINDUCTIVITY OF MULTISCALE COMPOSITES BASED ON POLY(LACTIDE-CO-GLYCOLIDE) ELECTROSPUN FIBERS EMBEDDED IN A GELATIN HYDROGEL. MATERIALS TODAY CHEMISTRY 2022, 24, 100804.

The final published version is available online at:
<https://doi.org/10.1016/j.mtchem.2022.100804>.

Terms of use:

Some rights reserved. The terms and conditions for the reuse of this version of the manuscript are specified in the publishing policy. For all terms of use and more information see the publisher's website.

This item was downloaded from IRIS Università di Bologna (<https://cris.unibo.it/>)

When citing, please refer to the published version.

Tantalum nanoparticles enhance the osteoinductivity of multiscale composites based on poly(lactide-co-glycolide) electrospun fibers embedded in a gelatin hydrogel

Anna Liguori^{a,§}, Maria Elena Gino^{a,§}, Silvia Panzavolta^{a,d}, Paola Torricelli^b, Melania Maglio^b, Annapaola Parrilli^c, Chiara Gualandì^{a,e}, Cristiana Griffoni^b, Giovanni Barbanti Brodano^b, Milena Fini^{b}, Maria Letizia Focarete^{a,d*}*

^aDepartment of Chemistry “Giacomo Ciamician” and INSTM UdR of Bologna, University of Bologna, via Selmi 2, 40126 Bologna, Italy.

^bIRCCS Istituto Ortopedico Rizzoli, Via di Barbiano 1/10, 40136 Bologna, Italy.

^cEmpa - Swiss Federal Laboratories for Materials Science and Technology, Center for X-ray Analytics - Überlandstrasse 129, 8600 Dübendorf, Switzerland.

^dHealth Sciences and Technologies – Interdepartmental Center for Industrial Research (HST-ICIR), Alma Mater Studiorum - Università di Bologna, 40064 Ozzano dell’Emilia, Bologna, Italy.

^eInterdepartmental Center for Industrial Research on Advanced Applications in Mechanical Engineering and Materials Technology, CIRI-MAM, University of Bologna, Viale Risorgimento, 2, 40136 Bologna, Italy.

KEYWORDS. Bone tissue regeneration, hydrogel/fibers composite scaffolds, tantalum nanoparticles, osteoinductive properties, bioactivity.

ABSTRACT

Bioresorbable polymeric materials have risen great interest as implants for bone tissue regeneration, since they show substantial advantages with respect to conventional metal devices, including biodegradability, flexibility, and the possibility to be easily modified to introduce specific functionalities. In the present work, an innovative nanocomposite scaffold, properly designed to show biomimetic and osteoinductive properties for potential application in bone tissue engineering, was developed. The scaffold is characterized by a multi-layer structure, completely different with respect to the so far employed polymeric implants, consisting in a poly(D,L-lactide-co-glycolide)/polyethylene glycol electrospun nanofibrous mat sandwiched between two hydrogel gelatin layers enriched with tantalum nanoparticles (NPs). The composition of the electrospun fibers, containing 10 wt% of polyethylene glycol, was selected to ensure a proper integration of the fibers in the gel phase, essential to endow the composite with flexibility and to prevent delamination between the layers. The scaffold maintained its structural integrity after 6 weeks of soaking in physiological solutions, albeit the gelatin phase was partially released. The combined use of gelatin, bioresorbable electrospun fibers and tantalum NPs endows the final device with biomimetic and osteoinductive properties. Indeed, results of the *in vitro* tests demonstrate that the obtained scaffolds clearly represent a favorable milieu for normal human bone-marrow derived mesenchymal stem cells viability and osteoblastic differentiation; moreover, inclusion of tantalum NPs in the scaffold improves cell performance with particular regard to early and late markers of osteoblastic differentiation.

1. Introduction

Bone injuries can be produced by several pathological conditions, and when they exceed the critical size of bone self-healing ability, an external intervention is required to promote bone regeneration and to restore normal bone function. The demand of new strategies and advanced materials for the healing and regeneration of bone tissue increases year by year, due to the population ageing. Devices for bone guided regeneration made of synthetic polymers including poly(lactide) (PLA), poly(glycolide) (PGA), and their copolymers poly(lactide-co-glycolide) (PLGAs) represent an encouraging solution for bone tissue engineering and bone substitutes and their features and requirements have been pointed out in a number of review papers[1- 3]. Good biocompatibility, proper mechanical properties, easy processing, suitable degradation rate and excellent osteoconductivity are the main characteristics of these classes of polymers.

The need for innovative devices able to enhance bone tissue regeneration led to the development of a new class of resorbable polymeric implants, that allow a better load-sharing between the implant and the bone and a greater transfer of load to the healing bone over time during their degradation [4,5]. Over the years, polyesters, mainly poly(α -hydroxy acids), like poly(lactic acid) (PLA), have been used for the preparation of bioresorbable implants tested *in vivo* for bone fixation and fusion applications [6-8], due to the possibility to be easily engineered to reach the desired mechanical properties and to their rather high resistance to hydrolytic degradation. The first published work in this frame dates back to 2002 and reported the *in vivo* testing of commercial bioresorbable PDLA implants, highlighting the lack of complications after a mean follow-up of 4.7 months [9]. In 2004, commercial PDLA implants packed with recombinant bone morphogenetic protein rhBMP2 were *in vivo* tested for single and multiple-level transforaminal lumbar interbody fusion procedure over a period of 18 months: an increase of the

fusion mass was observed over time, whereas the disc space height remained stable; no infections or complications related to the cages were detected [10]. More recently, a study, reporting a 5-7 years follow-up of patients treated with bioresorbable screws and plates made out of biodegradable copolymers composed of PLLA and PDLA, documented that cervical fusion was successfully achieved using these implants and the material brought out to be well tolerated by the patients [11].

Although the encouraging results, these commercial poly(α -hydroxy acids) scaffolds do not meet all the practical requirements coming from the medical field. Indeed, in order to be exploitable in the frame of bone tissue engineering, polymeric scaffolds need to show not only primary mechanical stability, rapid and high-quality bone ingrowth, modulable resorption rate, but also they are demanded to be endowed with osteoinductive properties, which are mandatory to reach the complete replacement of the implant with the generated bone tissue [12].

Osteoinductivity in polymeric scaffolds can be achieved through the release of bioactive compounds like BMP-2, growth factors such as the vascular or the basic fibroblast ones, and osteoinductive supplements such as platelets, which represent a valuable source of osteoinductive growth factors [13-18]. In addition, osteogenic supplements, including dexamethasone, ascorbic acid, vitamin D3, β -glycerol phosphate and l-proline, as the most efficient molecules, have been proposed [19].

In the present work, in order to overcome the limitations of conventional bioresorbable polymeric implants, we propose for the first time a multiscale composite material made of a microfibrinous mat sandwiched in a gelatin hydrogel enriched with well dispersed tantalum NPs as osteoinductive component. The novel hybrid scaffold is completely different in terms of structure and materials with respect to the so far employed resorbable polymeric implants and presents the flexibility and

the osteoinductive properties that are required for application in bone regeneration and treatment of bone defects. Poly(D,L-lactide-co-glycolide) (PLGA)/polyethylene glycol (PEG) mat were employed for electrospun mat production. PLGA (lactide:glycolide ratio 75:25 in mol), one of the most popular biodegradable polymers approved by the U.S. Food and Drug Administration [20], was selected for its biocompatibility, mechanical properties, rather high resistance to hydrolytic degradation [21,22]; however, due to the poor hydrophilicity of the PLGA electrospun mats, that prevents mat inclusion into the hydrogel, blends of PLGA/PEG at different composition were tested for the fabrication of the hybrid scaffold. The electrospun mat endows the scaffold with flexibility, while the hydrogel layers act as containment for the tantalum particles and as scaffold bioactive component. Gelatin was used as bioactive hydrogel material since, differently from collagen, it does not express antigenicity and it is completely biodegradable and biocompatible, as demonstrated by a wide range of applications in tissue engineering, drug delivery and gene therapy [23-28]. Tantalum, in the form of porous implants for orthopedic applications, was demonstrated to be bioactive, osteoinductive [29], and able to support the human osteoblast growth and differentiation better than titanium implants [30]. Tantalum NPs are currently used as nanoprobe for X-ray computed tomography imaging [31] and for drug delivery purposes [32]. However, to the best of our knowledge, they have been poorly investigated for bone tissue regeneration and only few papers report the combination of a polymeric materials with tantalum NPs [33,34].

2. Materials and methods

2.1 Materials

Poly(D,L-lactide-co-glycolide), PLGA, (lactide:glycolide=75:25, M_w =76000-15000 Da, RESOMER® RG 756 S, EVONIK); Polyethylene glycol, PEG, (M_w =1500 Da, Sigma Aldrich); Type A gelatin (300 Bloom, Sigma Aldrich) from pig skin; Genipin (Wako Chemicals) were used. Tantalum NPs (average particle size= 50-80 nm, purity >99%) was supplied by Io.li.tec Nanomaterials. Dichloromethane (DCM) and N,N-dimethylformamide (DMF) were purchased from Sigma-Aldrich and used without further purification.

2.2 Fabrication of electrospun mats

PLGA was dissolved in DCM/DMF (70/30 v/v) at a concentration of 20% w/v and stirred for 15 min at room temperature (RT). PEG was dissolved in double distilled water at a concentration of 65% w/v and stirred for 15 min at RT. Four distinct solutions, presenting weight ratios PLGA/PEG = 100/0, 95/5, 90/10, 80/20, were prepared and electrospun. The electrospinning process was carried out through a home-made electrospinning apparatus composed by a high voltage power supply (Spellman, SL 50 P 10/CE/230), a syringe pump (KD Scientific 200 series), a glass syringe containing the polymer solution, a stainless-steel blunt-ended needle (inner diameter= 0.5 mm) connected to the power supply and a grounded cylindrical aluminum collector (diameter = 5 cm, length= 10 cm, rotation angular speed = 70 rpm). The polymer solution was dispensed through a PTFE tube to the needle which was placed at a distance of 20 cm from the collector. The process was performed at RT and relative humidity of 50%, with a solution flow rate of 1.5 mL/h and an applied voltage of 18 kV DC. Mats with a thickness in the range 50 – 70 μ m were obtained and stored overnight in a desiccator to remove residual solvents.

2.3 Preparation of the hydrogels

Two distinct gelatin-based solutions were considered: (i) “gelatin solution”, containing Type A gelatin and genipin, used as crosslinking agent, and (ii) “gelatin-tantalum dispersion”, that, besides gelatin and genipin, also contains tantalum NPs. “Gelatin solution” was prepared as follows: (i) 2 grams of Type A gelatin were dissolved in double distilled water and kept under stirring at 42 °C for 30 min, (ii) 20 mg of genipin (2 wt% with respect to gelatin) were dissolved at 42 °C in phosphate-buffer saline (0.1 M, pH 7.4) and stirred for 30 min, (iii) the two solutions were mixed and kept under stirring at 42 °C for 25 min. “Gelatin-tantalum dispersion” was obtained by: (i) introducing 2 grams of gelatin and tantalum NPs (1 wt% with respect to gelatin), previously grinded, in double distilled water and keeping the mixture under stirring at 42 °C for 30 min, (ii) adding the “genipin solution” to the mixture, (iii) keeping the resulting dispersion under stirring at 42 °C for 25 min.

2.4 Preparation of hydrogel/fibers composite scaffolds

The procedure for the manufacturing of the PolyGelTa hydrogel/fibers composite scaffold is summarized in **Fig.1** “Gelatin-tantalum dispersion” at 42 °C (8 mL) was poured in a petri dish (inner diameter = 5.4 cm) and kept at 4 °C for 5 min to allow gel formation. Then the electrospun sample, cut from the mat in order to have a 5 cm diameter, was placed onto the gelatin layer. Additional 8 mL of “gelatin-tantalum dispersion” at 42 °C were poured onto the electrospun mat and the obtained material was kept at 4 °C for 24 h. Scaffolds were obtained from solvent casting method, after solvent evaporation for 24 h at RT under laminar flow. PolyGel composite scaffolds were produced by following the same procedure using the “gelatin solution” in place of the “gelatin-tantalum dispersion”.

2.5 Characterization methods

Thermogravimetric analysis (TGA) of the electrospun mats was carried out using a TA Instrument TGA Q500 analyzer from RT to 600 °C, with a heating rate of 10 °C/min in N₂ atmosphere. DSC measurements of the electrospun mats were carried out using a TA Instruments Q100 DSC apparatus in N₂ atmosphere from -90 °C to 120 °C with a heating scan rate of 20 °C/min; the T_g was taken at half-height of the glass transition heat capacity step in the second heating scan.

The morphology of the electrospun fibers and hydrogel/fibers composite scaffolds was investigated through a Philips XL20 Scanning Electron Microscope (SEM); samples were sputter-coated with gold prior to examination and the distribution of fiber diameters was determined through the measurement of about 250 fibers by means of image analysis software (ImageJ). Energy Dispersion X-ray Spectroscopy (EDS) of the hydrogel/fibers composite scaffolds was carried out by Inca X-sight SEM microscope at an accelerating voltage of 20 kV on Au coated samples; all the spectra were acquired by INCA software. Atomic Force Microscopy was performed to analyze the topography of the hydrogel/fibers composite scaffolds through a Park NX10 system equipped with PPP-NCHR tips (Nanosensors) and operating in non-contact mode.

Micro Computed Tomography analysis was carried out using the high-resolution microtomograph Skyscan 1172 (Bruker-MicroCT, Belgium) scanner applying a voltage of 60 kV and a current of 170 µA to the X-ray source. The samples were rotated 180° following 0.3° rotation steps. The scan images obtained, 2096 X 4000 pixels with a nominal resolution of 3.5 µm (pixel size), were then reconstructed with the NRecon program (version 1.7.1.6, Bruker) to obtain the microtomographic sections (4000 X 4000 pixels, maintaining the relative pixel size). For the reconstructions ring artefact reduction and beam hardening correction were used in

addition to the specific alignment relative to each individual scan. Using the reconstruction images, a 3D model was created with CTVox (Bruker microCT, Belgium) applying different thresholding to highlight the component materials according to their degree of X-ray absorption.

2.6 Determination of swelling degree and gelatin release.

The degree of swelling was measured after immersing the composite scaffolds in phosphate buffer (PB, 0.1 M, pH 7.4) for periods of time ranging from 1 min to 300 min. Wet samples were wiped with filter paper to remove excess liquid. The swelling was calculated according to

Equation 1.

$$swelling (\%) = \frac{w_w - w_d}{w_d} \cdot 100 \quad (1)$$

Where w_w and w_d are the weights of the wet and air-dried samples, respectively. For the gelatin release determination, 100 mg of the composite scaffolds were immersed in 5 mL of PB at 37 °C. For each time point (from 1 h to 43 days), PB was removed and replaced with fresh solution, 200 µL of the extracted solution were collected, incubated at 40 °C for 30 min and analyzed by means of a reaction with a bicinchoninic acid- copper (II) complex as previously described [26,28,35]. The concentration of released gelatin was determined at 562 nm by means of a Cary 1E Varian spectrophotometer through comparison with a calibration curve [36]. Each analysis was carried out in triplicate. The calibration curve was prepared by proper dilutions of a freshly prepared gelatin solution. The gelatin concentration was in the range 0.01 - 0.05 mg/mL.

2.7 *In vitro* test.

To assess the biological safety of the material, the first evaluation was a cytotoxicity test, performed by direct contact between the experimental materials and human osteoblast like cells

at short experimental time (72 h). Positive and negative controls were used. After assessment of negative cytotoxicity, an *in vitro* model for bioactivity was performed culturing human mesenchymal stem cells on biomaterials up to 14 days.

Cytotoxicity test: Human osteoblast-like cells MG63 (OB, Istituto Zooprofilattico Sperimentale IZSBS, Brescia, Italy) were cultured in DMEM medium (Dulbecco's Modified Eagle's Medium, Sigma, UK) supplemented with 10% FCS, and antibiotics (100 U/mL penicillin, 100 µg/mL streptomycin). Cells were detached from culture flasks by trypsinization, and cell number and viability were checked by trypan blue dye exclusion test. OB cells were plated at a density of 3×10^4 cells/mL in 24-well plates containing six sterile samples of PolyGel, and PolyGelTa. The same number of wells for negative (CTR–, DMEM only) and positive (CTR+, DMEM + 0.05% phenol solution) controls were also prepared. Plates were cultured in standard conditions, at 37 ± 0.5 °C with 95% humidity and $5\% \pm 0.2$ CO₂ up to 72 h. The quantitative evaluation of cytotoxicity was performed by measuring cell viability, and lactate dehydrogenase enzyme (LDH) release. Cell viability at 72 h was assessed by WST1 (WST1, Roche Diagnostics GmbH, Mannheim, Germany) colorimetric reagent test. The assay is based on the reduction of tetrazolium salt into a soluble formazan salt by a reductase of the mitochondrial respiratory chain, active only in viable cells. 100 µl of WST1 solution and 900 µl of medium (final dilution: 1:10) were added to the cell monolayer, and the multi-well plates were incubated at 37 °C for a further 4 h. Supernatants were quantified spectrophotometrically at 450 nm with a reference wavelength of 625 nm. Results of WST1 are reported as optical density (OD) and directly correlated with the cell number. Proliferation percent relative to CTR– at 24 h are also reported. At the end of experimental times the supernatant was collected from all wells and centrifuged to remove

particulates, if any, for LDH measure (LDH enzyme-kinetic test, Roche, D) according to manufacture instruction.

Bioactivity test - *in vitro* model: Normal human bone-marrow derived mesenchymal stem cells (hMSC, ATCC, VA, USA) at passage 2 were expanded in MSCBM (basal medium added with growth kit, ATCC). After a passage, cells were counted and seeded at concentration of 3×10^4 cells/mL in 24-well plates containing sterile samples of PolyGel, and PolyGelTa. The same number of wells were prepared for differentiated (CTRd) and undifferentiated (CTRnd) controls. Osteogenic differentiation medium was added to PolyGel, PolyGelTa and CTRd wells; fresh basal medium was used for CTRnd wells. Culture plates were maintained in standard conditions up to 14 days.

Bioactivity tests - cells viability and morphology: Evaluations were carried up at 3, 7, 10, and 14 days to assess cell viability and activity of hMSC on biomaterials and CTRs. Viability was measured by WST1 test and cells morphology was observed by Live/Dead® assay. A qualitative analysis for cell morphology was performed by Live/Dead® assay (Molecular Probes, Eugene, OR, USA), according to the manufacturer's instructions. Samples were visualized using an inverted microscope equipped with an epifluorescence setup (Eclipse TiU, NIKON Europe BV, NITAL SpA, Milan, Italy): excitation/emission setting of 488/530 nm to detect green fluorescence (live cells) and 530/580 nm to detect red fluorescence (dead cells). Alizarin Red staining was used to assess mineralization.

Bioactivity tests - gene expression: Bioactivity was studied by evaluating gene expression of the most common markers of osteoblastic differentiation on all groups. Total RNA was extracted from all samples at each experimental time using PureLink RNA Mini Kit (Life Technologies,

Carlsbad, CA, USA) and reverse transcribed with SuperScriptVILO cDNA Synthesis Kit (Life Technologies, Carlsbad, CA, USA), following the manufacturer instructions. Semi-quantitative polymerase chain reaction (PCR) analysis was performed for each sample in duplicate in a LightCycler 2.0 Instrument (Roche Diagnostics GmbH, Mannheim, Germany) using QuantiTect SYBR Green PCR Kit (Qiagen, Hilden, Germany) and gene-specific primers (Table S2). After melting curve analysis, to check for amplicon specificity, the threshold cycle was determined for each sample and relative gene expression was calculated using the 2-DDCt method. For each gene, expression levels were normalized to GAPDH (Glyceraldehyde 3-phosphate dehydrogenase) using undifferentiated cells (CTRnd) for each experimental time as calibrators.

Statistical analysis: Statistical evaluation of data was performed using the software package SPSS/PC+ Statistics TM 23.0 (SPSS Inc., Chicago, IL USA). The results presented are the mean of six independent values. Data are reported as mean \pm standard deviations (SD) at a significance level of $p < 0.05$. After having verified not normal distribution and homogeneity of variance, non-parametric tests were applied to detect significant differences among groups.

3 Results and discussion

The rationale of this work was to prepare innovative resorbable polymeric scaffolds potentially suitable in the framework of bone tissue regeneration. The scaffolds were obtained by combining the flexibility and hydrolytic resistance of PLGA electrospun mat with the biomimetic properties of gelatin crosslinked with genipin and the excellent bioactivity and osteoinductive properties of tantalum [29,30]. The composite scaffolds were composed by two external layers of gelatin hydrogel crosslinked with genipin and filled with tantalum NPs and an inner layer of PLGA

electrospun fibers, acting as reinforcing component (**Fig. 1c**) and are indicated as PolyGelTa. Identical scaffolds, with the same geometry but without tantalum NPs were also prepared (PolyGel). The preparation of the composite scaffolds was carried out according to the procedure reported in the Experimental Section. Briefly, it consisted in (i) placing the electrospun mat on the surface of a hydrogel layer obtained from a gelatin/tanipin solution containing tantalum NPs (gelatin-tantalum dispersion), (ii) pouring a second layer of gelatin-tantalum dispersion at 42 °C on the electrospun mat, (iii) storing the obtained material at 4 °C for 24 h (**Fig. 1a and b**). The same procedure was followed to prepare PolyGel composite scaffolds. The obtained scaffolds showed high flexibility and they were easy to handle and to bend (see **Video S1**, Supporting Information).

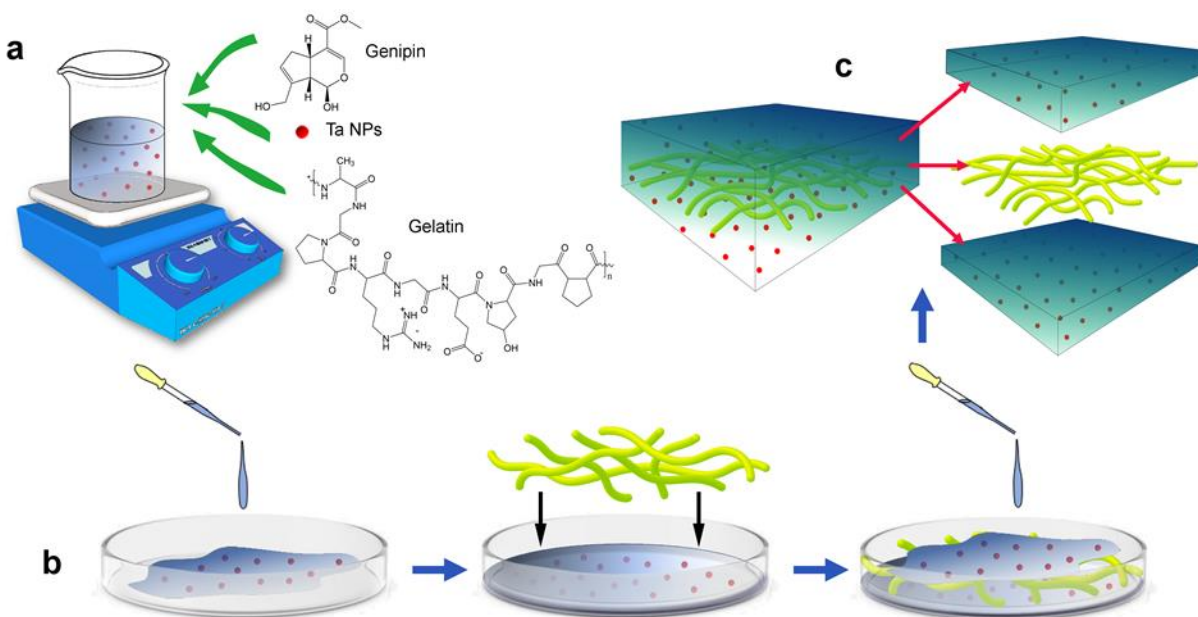


Fig. 1 Schematic illustration of the procedure for the fabrication of PolyGelTa hydrogel/fibers composite scaffold. (a) The gelatin-tantalum dispersion was stirred at 42 °C and 350 rpm; (b) 8 mL of the solution were poured in a petri dish, electrospun sample was placed onto the surface of

the solidified gelatin-based hydrogel and additional 8 mL of gelatin-tantalum dispersion at 42 °C were poured on the upper surface of the electrospun mat; (c) schematic structure of the final PolyGelTa scaffold.

For the preparation of the above composites, PLGA with lactide/glycolide molar ratio of 75/25 (PLGA 75:25) was selected on the basis of previous results on polymer degradation in physiological solution [21,22,37]. Due to the combination of the intrinsic hydrophobicity of the copolymer and thinly porous structure of the mat [38], PLGA 75:25 fibers are poorly wetted by water (**Fig. S1A**), thus hindering a good impregnation with the gelatin-based hydrogel, mandatory for achieving composite scaffolds with a good cohesion between layers. The design of composite scaffold formulation, therefore, required a preliminary optimization of fiber formulation by adding PEG to PLGA. Four distinct polymeric blend solutions, presenting weight ratios PLGA/PEG = 100/0, 95/5, 90/10, 80/20, were thus prepared and tested for electrospun mat preparation. As expected, the obtained mats, labelled PLGA/PEG0, PLGA/PEG5, PLGA/PEG10 and PLGA/PEG20, respectively, display a growing wettability with the increase in PEG content (**Fig. S1**), with the PLGA/PEG10 and PLGA/PEG20 being the more suitable formulations for ensuring a proper wettability during composite scaffold preparation.

The morphological analysis of the electrospun mats (**Fig. 2a-d**) revealed that the presence of PEG, at a concentration of 5%, 10% and 20% (w/w), did not significantly affect the fiber diameters ($(0.91 \pm 0.16) \mu\text{m}$ for PLGA/PEG0, $(1.16 \pm 0.22) \mu\text{m}$ for PLGA/PEG5, $(1.28 \pm 0.21) \mu\text{m}$ for PLGA/PEG10, $(1.32 \pm 0.20) \mu\text{m}$ for PLGA/PEG20), and all the mats showed a porous structure as well as smooth and bead free randomly oriented fibers. The presence of PEG is further confirmed by thermogravimetric analysis (TGA, **Fig. 2e** and **Fig. S2**), that enables to quantify the amount of PEG from the weight change at about 350°C, ascribable to PEG chain

degradation: 13 wt% for PLGA/PEG20, 7 wt% for PLGA/PEG10 and 4 wt% for PLGA/PEG5, rather close to the feed ones.

Beside wettability, polymer glass transition temperature (T_g) was the other fundamental property to be considered for successfully preparing our composite scaffolds. Indeed, to preserve the fibrous morphology during the scaffolds fabrication procedure the fibrous mat must thermally resist to the contact with the gelatin/genipin solution kept at 42°C. On this basis, results of Differential Scanning Calorimetry (DSC) analysis (**Fig. 2f** and **Table S1**) led to exclude PLGA/PEG20 as possible formulation for the scaffold production: the presence of PEG, that acts as plasticizer for PLGA, causes a dramatic decrease of T_g from 53°C (T_g of PLGA/PEG0) to 26°C (T_g of PLGA/PEG20). Conversely, both PLGA/PEG5 and PLGA/PEG10 with T_g of 43°C and 40°C, respectively, turned out to be suitable for the composite scaffolds production.

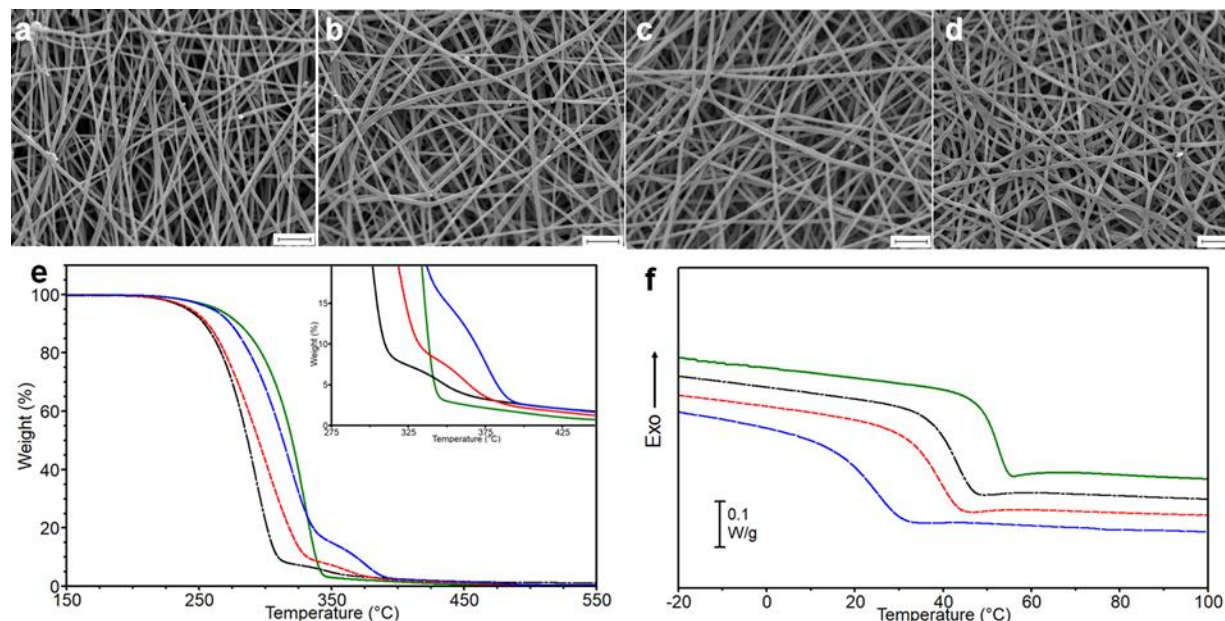


Fig. 2. SEM micrographs of the electrospun mats: (a) PLGA/PEG0, (b) PLGA/PEG5, (c) PLGA/PEG10, (d) PLGA/PEG20 (scale bar = 10 μm). (e) TGA curves, and (f) DSC curves:

PLGA (green solid line), PLGA/PEG5 (black broken dashed line), PLGA/PEG10 (red short dashed line), PLGA/PEG20 (blue long dashed line).

Nevertheless, due to the poor wettability of PLGA/PEG5 (**Fig. S1b**), PLGA/PEG10 was selected for the preparation of the hydrogel/fibers composite scaffolds. The amount of PEG in PLGA/PEG10 endowed the mats with hydrophilic properties and enabled its excellent impregnation with the gelatin-based hydrogel, as confirmed by the SEM cross-sectional view of PolyGelTa in **Fig. 3a-b**, where it is evident that the hydrogel completely fills the pores of the PLGA/PEG10 mat without affecting the fibrous texture. Conversely, the cross-sectional view of PolyGelTa fabricated by using PLGA/PEG0 fibers, showed the poor impregnation of the mat by the hydrogel (**Fig. 3c-d**), thus confirming our findings.

The tomographic analysis (**Fig. 3e-g**) highlighted the presence of well dispersed tantalum NPs (red spots) throughout the thickness of both the hydrogel layers of PolyGelTa and at the surface (**Fig. 3e-f** and **Fig. S3**), and the lack of relevant aggregates in agreement with the chemical characterization performed through EDS (**Fig. S4**). Moreover, the analysis of the distribution of the nanoparticles along the thickness of the hydrogel layers documented that they are well distributed, highlighting the hydrogel's effectiveness to prevent their aggregation (**Fig. S5**). This result can be interpreted considering a stabilization of tantalum NPs by means of gelatin chains due to electrostatic interactions. In fact, Type A gelatin used in this work has an isoelectric pH of 8.4, meaning that the biopolymer is positively charged under the composite preparation conditions (measured pH= 7.2) while tantalum NPs might be negatively charged at this pH value, as suggested in literature [39]. Rapid gelation of the hydrogel further stabilizes the nanoparticles dispersion, thus preventing aggregation phenomena, which is one of the main issues to be considered during the preparation process of nanocomposite hydrogels [40, 41] The findings on

homogeneous tantalum NPs dispersion were further confirmed by the topographic characterization of the composite surfaces by means of atomic force microscopy (**Fig. 3h-i**); indeed, a significant higher roughness, ascribable to the presence of tantalum NPs, was observed for PolyGelTa compared with PolyGel, thus allowing to exclude the presence of aggregates, typical of the as supplied tantalum NPs (**Fig. S6**). Roughness has been documented to significantly affect cell behavior and performance [42]: cells preferentially adhere, spread, migrate, and proliferate on rough surfaces than on smooth ones [43,44]. In light of this aspect, composite scaffolds containing tantalum NPs should represent a better milieu for bone cell residence and function as well as for the bone matrix formation [45].

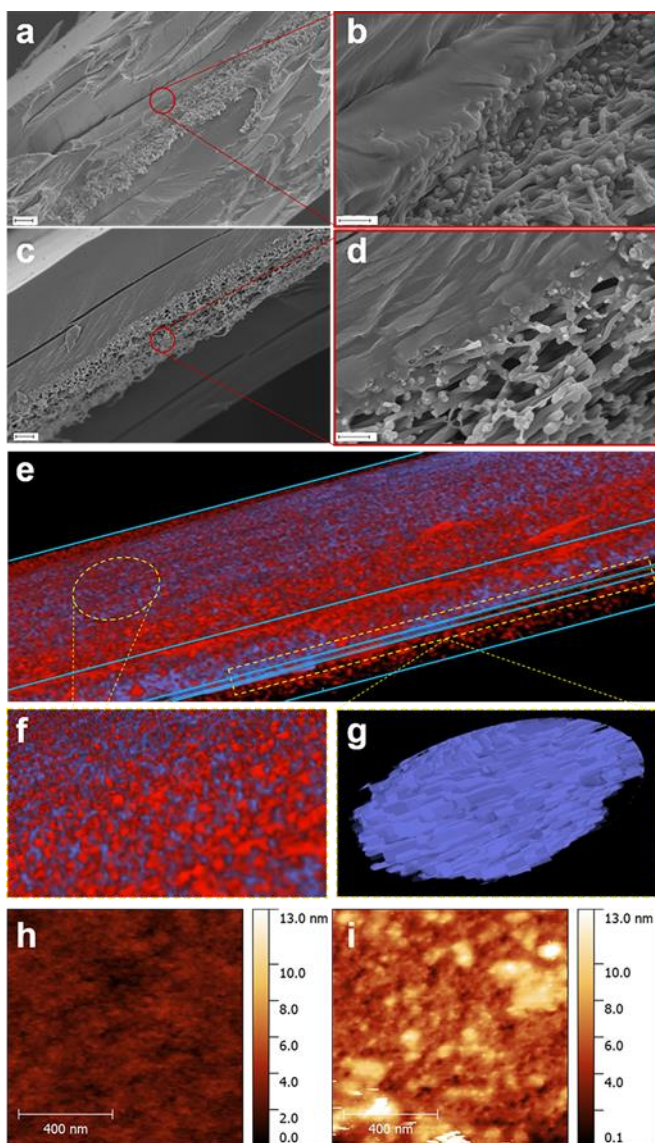


Fig. 3. SEM micrographs of hydrogel/fibers composite scaffolds of PolyGelTa fabricated by using (a-b) PLGA/PEG10 mat, and (c-d) PLGA/PEG0. Scale bars: (a-c) 20 μm, (b-d) 5 μm. μCT imaging of PolyGelTa: surface and cross-section view showing: (e) tantalum NPs in red and polymeric fibers in blue; (f) magnification of a portion of surface area, and (g) reconstruction of the electrospun mat included between the hydrogel layers. Atomic force microscope analysis of the surface of (h) PolyGel, and (i) PolyGelTa. Video of μCT is available in **Video S2**, Supporting Information.

PolyGel and PolyGelTa swelled in phosphate buffer (PB) neither breaking nor splitting. As reported in **Fig. 4a**, the swelling degree of both scaffolds quickly increased during the first 60 min of immersion in PB to around 160% and 170% for PolyGel and PolyGelTa, respectively, whereas the successive increase with time turned out to be rather modest. Both the scaffolds, after 300 min of immersion, showed a comparable swelling degree, increasing their weight up to around 250%. Concerning the gelatin release, shown in **Fig. 4b**, no significant differences were detected among PolyGel and PolyGelTa for all the immersion times in PB: after 14 days of immersion, a small weight loss (around the 10%) was observed; on increasing the immersion time the weight loss significantly increased, reaching values around 30-40% after 43 days of immersion. This weight loss can be primarily ascribed to a progressive release of gelatin from the gel component, while a significant PEG release from the fibrous component can be excluded from the results of TGA analysis carried out on PLGA/PEG10 mat after 7 days of immersion in PB (**Fig. S7**). The mat did not show significant variations of the composition with respect to the as-spun mat, although a very modest dissolution of PEG with the increase of the soaking time up to 14 days can be noticed.

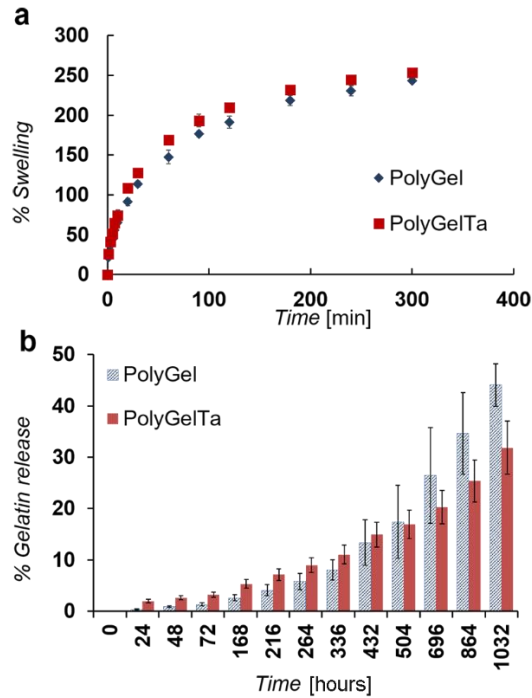


Fig. 4. (a) Swelling, and (b) gelatin release curves of PolyGel and PolyGelTa in PB.

Since the new composite scaffold has been designed for bone tissue contact, MG63 osteoblast-like cell line was used for the cytotoxicity test. The quantitative evaluation of cytotoxicity was performed by measuring cell viability and lactate dehydrogenase enzyme (LDH) release. Cell viability is considered a fundamental parameter of evaluation, as reduction of viability by more than 30% is considered a cytotoxic effect. Results of cell viability after 3 days of culture (**Fig. 5**) showed values for PolyGel and PolyGelTa not different from CTR-. CTR+ was significantly lower than all other groups.

LDH dosage is an indirect parameter of cytotoxicity, because its release is due to a damage of cell membranes. LDH measure (**Fig. 5b**) was in line with cell viability, showing low concentration of LDH in cell culture in PolyGel, PolyGelTa and CTR- groups, significantly different from high values of CTR+ (Pearson inverse correlation WST1/LDH -0.969, $p < 0.005$).

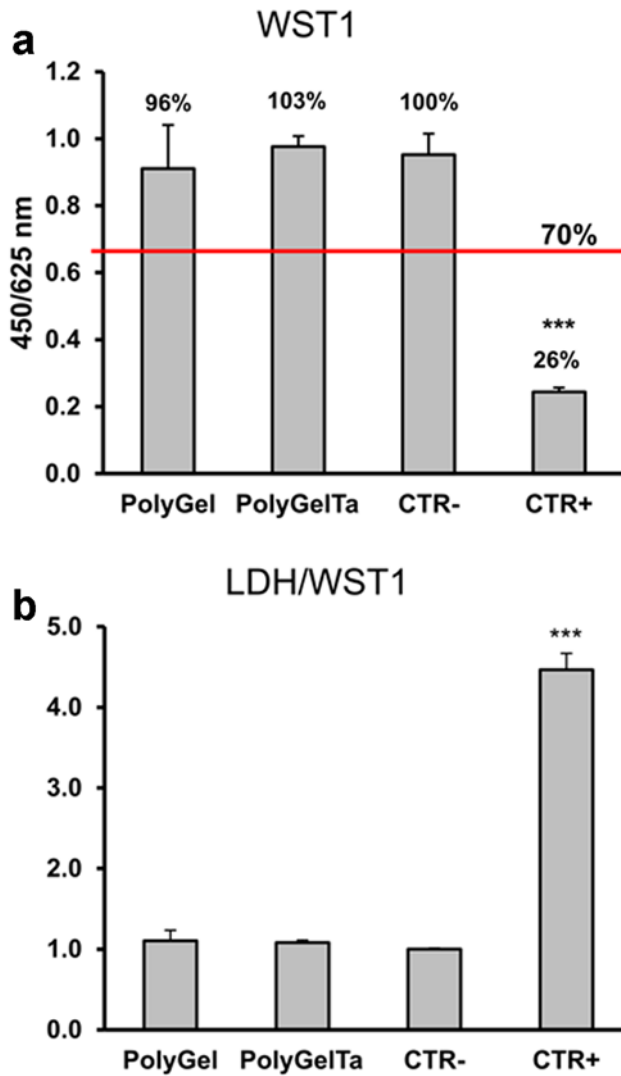


Fig. 5. Cytotoxicity test after 3 days of culture. (a) Cell viability by WST1 test (red line representing 70% cell viability, reference limit for cytotoxicity), and (b) LDH measure.

***CTR+ versus PolyGel, PolyGelTa, CTR- (p<0.0005).

To investigate the capability of PolyGel and PolyGelTa to act as support for cell growth and for maintenance of differentiation, bone-marrow derived mesenchymal stem cells (hMSC) were chosen after verifying their ability to differentiate toward osteoblastic lineage. Cells culture in

basic and differentiating medium were compared for cell viability, and ability to mineralize, by means of Live&Dead, and Alizarin red staining, respectively (**Fig. 6a-b**). Live&Dead fluorescent staining is useful to observe cell morphology, attachment, and scaffold colonization. hMSC showed regular morphology in both conditions: cells had well defined shapes and were spread onto the surface. Differences in shapes and orientation are notable between differentiated and undifferentiated cells. Alizarin red staining, that is used to evaluate calcium deposition, confirmed osteoblastic differentiation showing many foci of mineralization, that were already present after 1 week and were well evident after 2 weeks of culture.

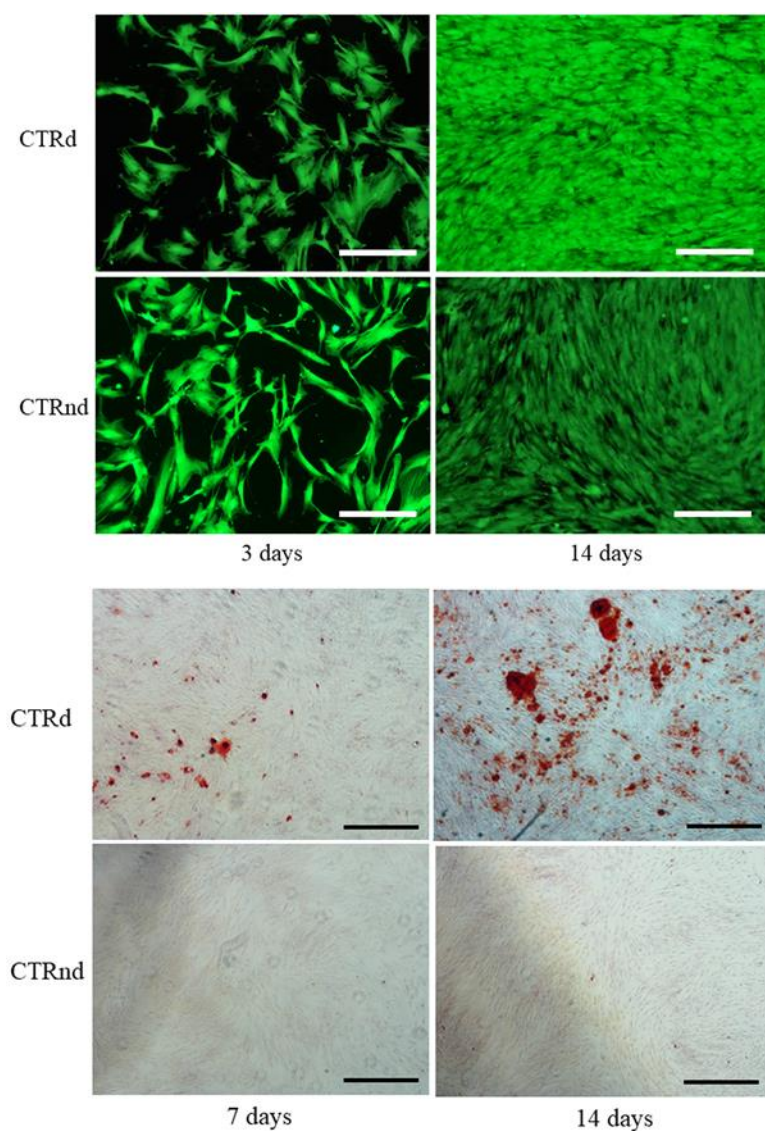


Fig. 6. hMSC differentiated and undifferentiated control cultures (CTRd and CTRnd respectively). (a) Live&Dead fluorescent staining (10x), scale bar = 100 μm ; (b) Alizarin Red staining (4x), scale bar = 500 μm . Both staining demonstrated the differences between differentiated and not differentiated cells, as shape and orientation (a), and calcium deposition (b).

In order to investigate the potential of the scaffolds in inducing and supporting a fast cell colonization, viability and bioactivity of hMSC cultured on PolyGel and PolyGelTa were

evaluated at 3, 7, 10 and 14 days of culture. Results were compared with differentiated (CTRd) and undifferentiated (CTRnd) cultures. hMSC grown on biomaterials showed a lower proliferation when compared to CTRd (PolyGel at each experimental time, PolyGelTa at 3, 10 and 14 days), but the percentage of viability was always over 70%, confirming the absence of cytotoxicity (**Fig. 7a**). Live&Dead staining as well demonstrated that hMSC adhered and grew onto PolyGel and PolyGelTa samples, showing regular morphology and full colonization of biomaterial surface (**Fig. 7b**). Images are consistent with WST1 values. SEM analysis performed onto PolyGelTa after cell colonization confirmed these results (**Fig. S8**).

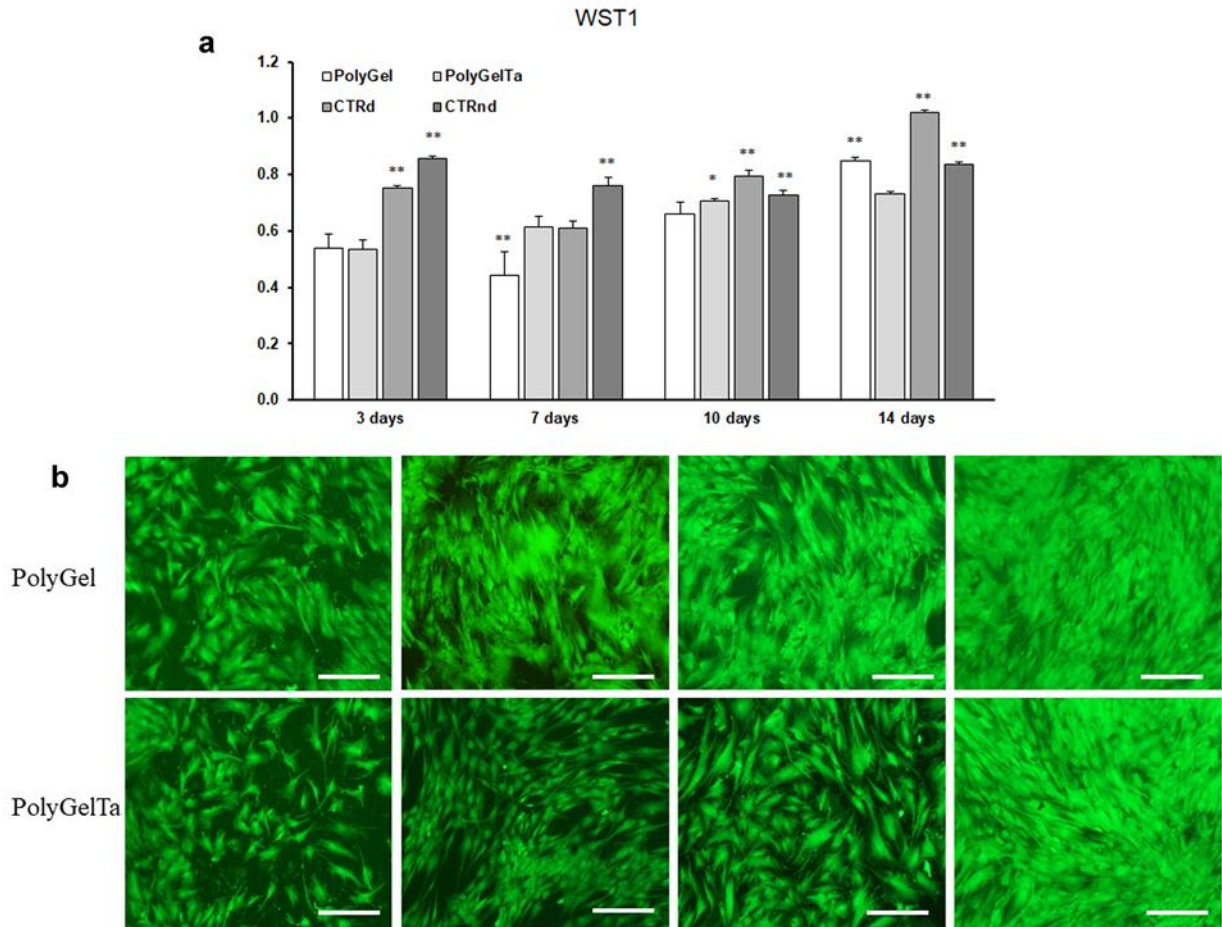


Fig. 7. hMSC cultured on PolyGel and PolyGelTa and CTRs at 3, 7 10, 14 days of culture. (a) Cells viability by WST1 test; (b) Live&Dead fluorescent staining of cells grown on biomaterials: hMSC cultured onto PolyGel (upper row) and PolyGelTa (lower row) at the same experimental points; scale bar = 100 μ m (10x). Statistical analysis is reported in the figure (* $p < 0.05$, ** $p < 0.005$). 3days: **CTRd, CTRnd vs PolyGel, PolyGelTa; **CTRd vs CTRnd. 7 days: **PolyGel vs PolyGelTa, CTRd, CTRnd; **CTRnd vs PolyGelTa, CTRd; 10days: *PolyGelTa vs PolyGel; **CTRd vs PolyGel, PolyGelTa, CTRnd; **CTRnd vs PolyGel, PolyGelTa. 14days: **PolyGel, CTRnd vs PolyGelTa; **CTRd vs PolyGel, PolyGelTa, CTRnd.

Common marker genes of osteoblasts for osteogenic differentiation or involved in the differentiating process were evaluated at 3, 7, 10, and 14 days, in biomaterials and controls, to assess if hMSC cultured on PolyGel and PolyGelTa were active and maintained the induced differentiation (**Fig. 8a-b**). RUNX2 and CtSP7/Osterix were chosen as gene expression of mesenchymal stem cell differentiation toward osteoblastic lineage. They are key transcription factors that play a role in early and late osteoblastic differentiation, respectively. In particular, RUNX2 is responsible for inducing hMSC to differentiate into osteoblastic cells. CtSP7/Osterix acts subsequently for maintaining a mature state of cells and its activation favors healing fracture or implant osteointegration. ALPL, COL1A1 and BGLAP represent the typical product of activity of differentiated osteoblast, namely alkaline phosphatase, collagen type I and Osteocalcin, that contribute to extracellular matrix deposition and to tissue mineralization.

The comparison between CTRnd and CTRd demonstrated that hMSC were able to differentiate when cultured in the appropriate conditions: results of all studied parameters at all experimental time of CTRd were higher and significantly different from CTRnd (**Fig. 8a**), apart from transient lower values of BGLAP and CtSP7 at 7 days. Results of PolyGel, PolyGelTa and CTRd at 7 and

14 days of culture were reported in **Fig. 8b** in function of CTRnd, considered as 1. These results were particularly significant because they showed that all gene expressions observed were highly enhanced by the culture with PolyGel. Moreover, the presence of tantalum positively influenced cell behavior: hMSC cultured on PolyGel and PolyGelTa were strongly activated in the early stage of cell differentiation, as showed by very high expression of ALPL and RUNX2. Collagen type I and Osteocalcin genes were also greatly stimulated, showing that the cells expressed the typical markers of differentiated osteoblasts, with production of Osteocalcin and deposition of collagen for the formation of the extracellular matrix. At 14 days CtSP7 was particularly enhanced, confirming the maintenance of osteoblastic phenotype.

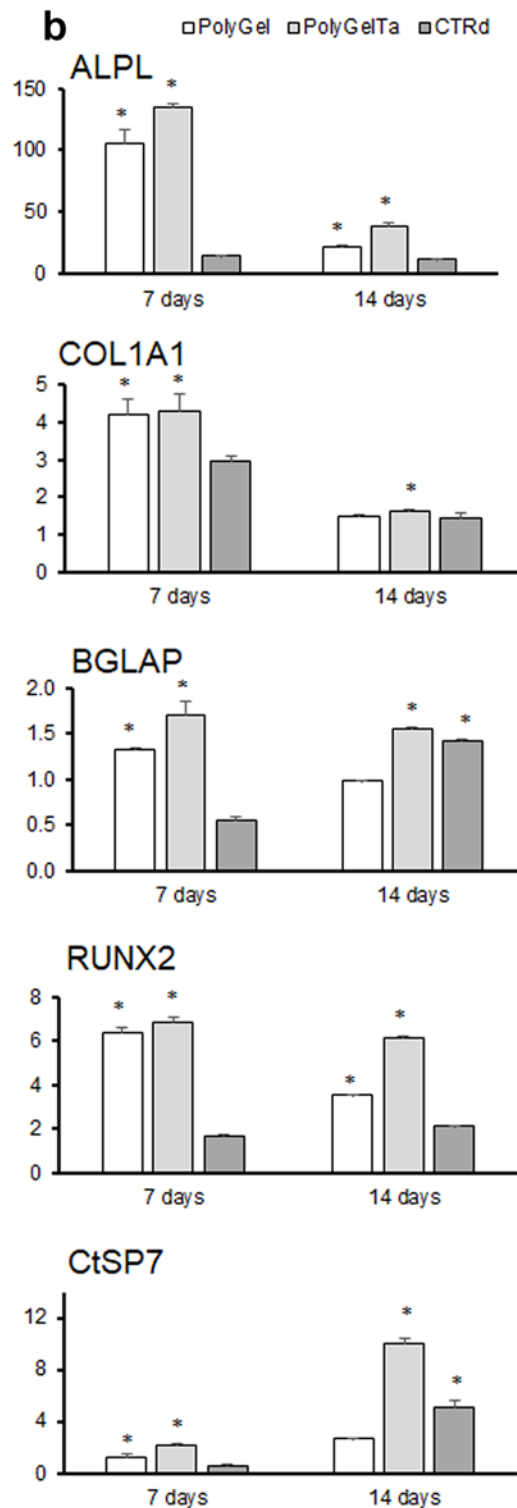
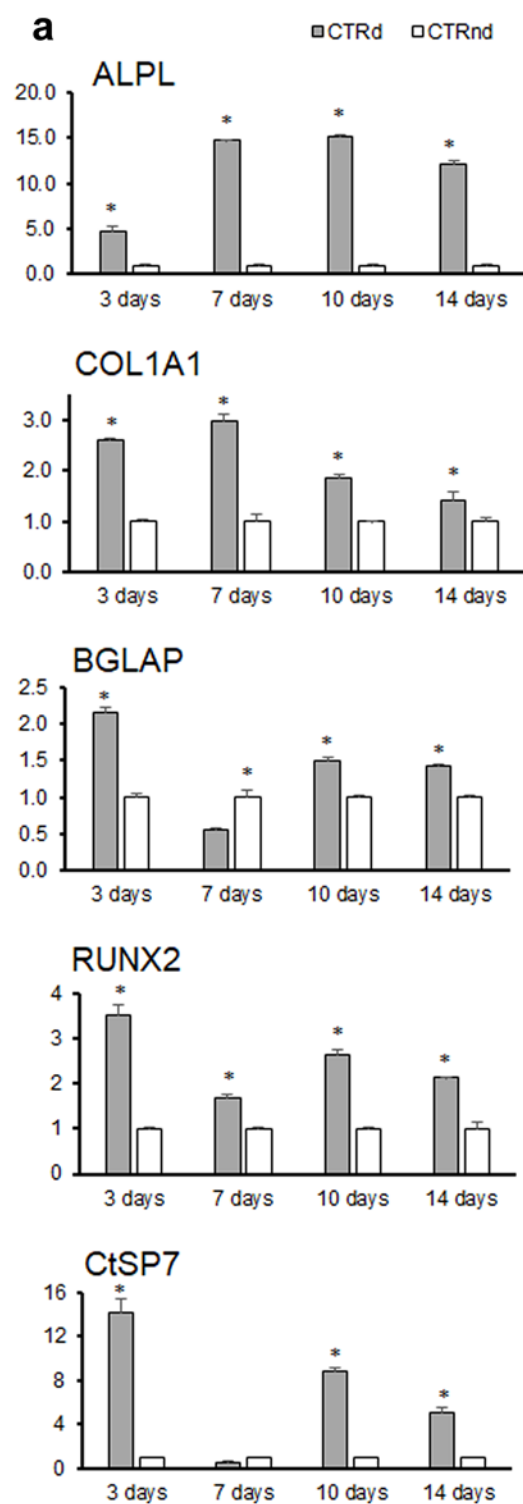


Fig. 8. Gene expression of main markers of osteoblast differentiation in (a) undifferentiated (CTRnd) and differentiated (CTRd) hMSC control cultures from 3 to 14 days of culture, and (b) in biomaterials compared to CTRd at 7 and 14 days of culture. All results were normalized to CTRnd. Statistical analysis is reported in the figure (* $p < 0.05$). a) *CRTd vs CTRnd. b) ALPL, BGLAP, RUNX2, CtSP7: 7, 14 days *PolyGelTa vs PolyGel, CTRd; *PolyGel vs CTRd. COL1A1: 7 days *PolyGel, PolyGelTa vs CTRd; 14 days *PolyGelTa vs PolyGel, CTRd.

4. Conclusions

In this work, an innovative hydrogel/fibers nanocomposite scaffold showing interesting properties for application in bone tissue regeneration, such as flexibility, biodegradability, biocompatibility, biomimetics and osteoinduction, is developed. The scaffolds were obtained by placing an electrospun mat, obtained from a blend solutions of PLGA:PEG=90:10 w/w, between two gelatin-based hydrogel containing tantalum NPs as osteoinductive component. The materials characterization highlighted that the fibrous mat was well impregnated by the hydrogel and the presence of the tantalum NPs led to a significant increase of the scaffold surface roughness, due to the presence of dispersed particles and aggregates, that was previously reported to have a positive effect on cell adhesion, migration and proliferation. Scaffolds are able to maintain their layered structure over time: in fact, no delamination between the fibrous mat and the gelatin hydrogels was observed after six weeks in physiological conditions. Cytotoxicity evaluation demonstrated that both PolyGel and PolyGelTa allow cell viability and spreading, and hMSC were used to evaluate the potential of scaffold to stimulate their differentiation toward the osteoblastic lineage. All results of *in vitro* study clearly demonstrated that PolyGel is an

appropriate substrate to support hMSC viability and osteoblastic differentiation and that the addition of tantalum enhances cell performances. The proposed layered scaffold, obtained from bioresorbable polymeric materials, represents a promising approach for the treatment of bone defects, due to its versatility in functional properties and its capability to overcome the typical issues of conventional metal devices, such as non-degradability and remarkably different mechanical properties with respect to the bone.

ASSOCIATED CONTENT

Supporting Information

Water absorption analysis; TGA derivative curves; DSC results; EDX results; TEM images of tantalum nanoparticles; TGA of the composites before and after soaking in PB; SEM of cells colonizing the scaffold; Specification of primer used for qPCR analysis; video showing scaffold's flexibility; video of the μ -CT analysis.

AUTHOR INFORMATION

Corresponding Authors

§ These authors contributed equally to this work.

***Milena Fini** - *IRCCS Istituto Ortopedico Rizzoli, Via di Barbiano 1/10, 40136 Bologna, Italy*
Email: milena.fini@ior.it

***Maria Letizia Focarete** – *Department of Chemistry “Giacomo Ciamician” and INSTM UdR of Bologna, and Health Sciences and Technologies – Interdepartmental Center for Industrial Research (HST-ICIR), Alma Mater Studiorum - Università di Bologna, 40126 Italy.*
Email: marialetizia.focarete@unibo.it

Author Contributions

Anna Liguori: Conceptualization, Methodology, Writing- Original draft preparation, Writing- Reviewing and Editing. Maria Elena Gino: Conceptualization, Methodology, Data curation, Writing- Original draft preparation. Silvia Panzavolta: Conceptualization, Methodology, Data

curation, Supervision, Writing- Original draft preparation, Writing- Reviewing and Editing. Paola Torricelli: Methodology, Data curation, Writing- Original draft preparation. Melania Maglio: Data curation, Writing- Original draft preparation. Annapaola Parrilli: Data curation, Writing- Original draft preparation. Chiara Gualandi: Methodology, Writing- Reviewing and Editing. Cristiana Griffoni: Methodology, Data curation, Writing- Original draft preparation. Giovanni Barbanti Brodano: Supervision, Writing- Reviewing and Editing. Milena Fini: Conceptualization, Methodology, Supervision, Writing- Reviewing and Editing. Maria Letizia Focarete: Conceptualization, Methodology, Supervision, Writing- Reviewing and Editing.

ACKNOWLEDGMENT

The Italian Ministry of University and Research (MIUR) is acknowledged. Authors are grateful to IRCCS Istituto Ortopedico Rizzoli (funds Ministero della Salute – Ricerca Corrente).

Data availability

The raw/processed data required to reproduce these findings cannot be shared at this time due to technical and time limitations.

REFERENCES

- [1] P. Lichte, H. C. Pape, T. Pufe, P. Kobbe, H. Fischer, Scaffolds for bone healing: concepts, materials and evidence, *Injury, Int. J. Care Injured*, 42(6), (2011), 569-573, <https://doi.org/10.1016/j.injury.2011.03.033>
- [2] C. Liu, Z. Xia, J.T. Czernuszka, Design and development of three-dimensional scaffolds for tissue engineering, *Chemical Engineering Research and Design*, 85(7), (2007) 1051-1064, <https://doi.org/10.1205/cherd06196>
- [3] Y. Liu, J. Lim, S. H. Teoh, Review: development of clinically relevant scaffolds for vascularised bone tissue engineering, *Biotechnology advances*, 31(5), (2013) 688–705, <https://doi.org/10.1016/j.biotechadv.2012.10.003>

- [4] J. Li, L. Qin, K. Yang, Z. Ma, Y. Wang, L. Cheng, D. Zhao, Materials evolution of bone plates for internal fixation of bone fractures: A review, *Journal of Materials Science & Technology* 36 (2020) 190–208, <https://doi.org/10.1016/j.jmst.2019.07.024>
- [5] P. I. J. M. Wuisman, T. H. Smit, Bioresorbable polymers: heading for a new generation of spinal cages, *Eur. Spine J.* 15 (2) (2006) 133–148, <https://doi.org/10.1007/s00586-005-1003-6>
- [6] A. U. Daniels, M. K. Chang, K. P. Andriano, Mechanical properties of biodegradable polymers and composites proposed for internal fixation of bone, *J Appl Biomater*, 1 (1) (1990) 57–78, <https://doi.org/10.1002/jab.770010109>
- [7] J. L. Katz, C. G. Ambrose, C. McMillin, P. Spencer, In: Wnek GE, Bowlin GL (eds) *Encyclopedia of biomaterials and biomedical engineering*, 2004, Marcel Dekker, New York, pp 1160–1171.
- [8] M. Vert, In: Wnek GE, Bowlin GL (eds) *Encyclopedia of biomaterials and biomedical Engineering*, 2004, Marcel Dekker, New York, pp 1254–1264.
- [9] T. G. Lowe, J. D. Coe, Bioresorbable polymer implants in the unilateral transforaminal lumbar interbody fusion procedure, *Orthopedics* 25 (10) (2002) S1179–83, <https://doi.org/10.3928/0147-7447-20021002-09>.
- [10] T. R. Kuklo, M. K. Rosner, D. W. Polly, Computerized tomography evaluation of a resorbable implant after transforaminal lumbar interbody fusion, *Neurosurg. Focus.* 16 (3) (2004) E10, <https://doi.org/10.3171/foc.2004.16.3.11>
- [11] V. Rodrigo, A. Maza, J. B. Calatayud, L. Bances, F. J. Diaz, M. J. Gimeno, B. Carro, Long-term follow-up of anterior cervical discectomy and fusion with bioabsorbable plates and screws, *Clin. Neurol. Neurosurg.* 136 (2015) 116–121, <https://doi.org/10.1016/j.clineuro.2015.04.002>

- [12] Y. Shikinami, M. Okuno, Mechanical evaluation of novel spinal interbody fusion cages made of bioactive, resorbable composites, *Biomater.* 24 (18) (2003) 3161-3170, [https://doi.org/10.1016/S0142-9612\(03\)00155-8](https://doi.org/10.1016/S0142-9612(03)00155-8)
- [13] M. Rampichová, M. Buzgo, A. Míčková, K. Vocetková, V. Sovková, V. Lukášová, E. Amler, Platelet-functionalized three-dimensional poly- ϵ -caprolactone fibrous scaffold prepared using centrifugal spinning for delivery of growth factors, *International journal of nanomedicine*, 12, (2017), 347, <https://doi.org/10.2147/IJN.S120206>
- [14] L. Yin, S. Yang, M. He, Y. Chang, K. Wang, Y. Zhu, Y. Yu, Physicochemical and biological characteristics of BMP-2/IGF-1-loaded three-dimensional coaxial electrospun fibrous membranes for bone defect repair, *Journal of Materials Science: Materials in Medicine*, 28(6), (2017), 94, <https://doi.org/10.1007/s10856-017-5898-3>
- [15] H. Zhang, J. Liang, Y. Ding, P. Li, The controlled release of growth factor via modified coaxial electrospun fibres with emulsion or hydrogel as the core, *Materials Letters*, 181, (2016) 119-122, <https://doi.org/10.1016/j.matlet.2016.05.146>
- [16] M. Rubert, J. Dehli, Y. F. Li, M. B. Taskin, R. Xu, F. Besenbacher, M. Chen, Electrospun PCL/PEO coaxial fibers for basic fibroblast growth factor delivery, *Journal of Materials Chemistry B*, 2(48), (2014), 8538-8546, <https://doi.org/10.1039/C4TB01258E>
- [17] E. Prosecká, M. Rampichová, A. Litvinec, Z. Tonar, M. Králíčková, L. Vojtová, E. Amler, Collagen/hydroxyapatite scaffold enriched with polycaprolactone nanofibers, thrombocyte-rich solution and mesenchymal stem cells promotes regeneration in large bone defect in vivo, *Journal of Biomedical Materials Research Part A*, 103(2), (2015), 671-682, <https://doi.org/10.1002/jbm.a.35216>

- [18] M. Buzgo, M. Rampichova, K. Vocetkova, V. Sovkova, V. Lukasova, M. Doupnik, E. Amler, Emulsion centrifugal spinning for production of 3D drug releasing nanofibres with core/shell structure. *RSC advances*, 7(3), (2017), 1215-1228, DOI: 10.1039/C6RA26606A
- [19] L. Vera, B. Matej, V. Karolina, K. Tereza, T. Zbyněk, D. Miroslav, R. Michala, Osteoinductive 3D scaffolds prepared by blend centrifugal spinning for long-term delivery of osteogenic supplements. *RSC advances*, 8(39), (2018), 21889-21904, <https://doi.org/10.1039/C8RA02735H>
- [20] K. H. Hong, S. H. Woo, T. J. Kang, In vitro degradation and drug-release behavior of electrospun, fibrous webs of poly(lactic-co-glycolic acid), *J. Appl. Polym. Sci.* 124 (1) (2012) 209-214, <https://doi.org/10.1002/app.33357>
- [21] L. Lu, C. A. Garcia, A. G. Mikos, In vitro degradation of thin poly(DL-lactic-co-glycolic acid) films, *J. Biomed. Mater. Res* 46 (2)(1999) 236-244, [https://doi.org/10.1002/\(SICI\)1097-4636\(199908\)46:2<236::AID-JBM13>3.0.CO;2-F](https://doi.org/10.1002/(SICI)1097-4636(199908)46:2<236::AID-JBM13>3.0.CO;2-F)
- [22] L. Wu, J. Ding, In vitro degradation of three-dimensional porous poly (D, L-lactide-co-glycolide) scaffolds for tissue engineering, *Biomater.* 25 (27) (2004)5821-5830, <https://doi.org/10.1016/j.biomaterials.2004.01.038>
- [23] J. Aduba, J. A. Hammer, Q. Yuan, A. Yeudall, G. L. Bowlin, H. Yang, Semi-interpenetrating network (sIPN) gelatin nanofiber scaffolds for oral mucosal drug delivery, *Acta Biomater* 9 (5) (2013)6576-6584, <https://doi.org/10.1016/j.actbio.2013.02.006>
- [24] M. Angarano, S. Schulz, M. Fabritius, R. Vogt, T. Steinberg, P. Tomakidi, C. Friedrich, R. Mulhaupt, Layered gradient nonwovens of in situ crosslinked electrospun collagenous nanofibers

- used as modular scaffold systems for soft tissue regeneration, *Adv. Funct. Mater.* 23 (26) (2013) 3277-3285,. <https://doi.org/10.1002/adfm.201202816>
- [25] M. Li, M. J. Mondrinos, M. R. Gandhi, F. K. Ko, A. S. Weiss, P. I. Lelkes, Electrospun protein fibers as matrices for tissue engineering, *Biomaterials* 26 (30) (2005) 5999-6008, <https://doi.org/10.1016/j.biomaterials.2005.03.030>
- [26] S. Panzavolta, M. Gioffrè, M. L. Focarete, C. Gualandi, L. Foroni, A. Bigi, Electrospun gelatin nanofibers: optimization of genipin cross-linking to preserve fiber morphology after exposure to water, *Acta Biomater.* 7 (4) (2011)1702-1709,<https://doi.org/10.1016/j.actbio.2010.11.021>
- [27] J. F. Mano, R. L. Reis, Osteochondral defects: present situation and tissue engineering approaches, *J. Tissue Eng. Regen. Med.* 1 (4) (2007) 261- 273, <https://doi.org/10.1002/term.37>
- [28] L. S. Dolci, A. Liguori, S. Panzavolta, A., Misericocchi, N. Passerini, M. Gherardi, V. Colombo, A. Bigi, B. Albertini, Non-equilibrium atmospheric pressure plasma as innovative method to crosslink and enhance mucoadhesion of econazole-loaded gelatin films for buccal drug delivery, *Colloids Surf B Biointerfaces* 163 (2018) 73-82, <https://doi.org/10.1016/j.colsurfb.2017.12.030>
- [29] M. M. Lu, P. S. Wu, X. J. Guo, L. L. Yin, H. L. Cao, D. Zou, Osteoinductive effects of tantalum and titanium on bone mesenchymal stromal cells and bone formation in ovariectomized rats, *Eur. Rev. Med. Pharmacol. Sci.* 22 (21) (2018) 7087-7104, https://doi.org/10.26355/eurev_201811_16241
- [30] B. R. Levine, S. Sporer, R. A. Poggie, C. J. Della Valle, J. J. Jacobs, Experimental and clinical performance of porous tantalum in orthopedic surgery, *Biomaterials* 27 (27) (2006) 4671-4681, <https://doi.org/10.1016/j.biomaterials.2006.04.041>

- [31] P. J. Bonitatibus, A. S. Torres, B. Kandapallil, B. D. Lee, G. D. Goddard, R. E. Colborn, M. E. Marino, Preclinical assessment of a zwitterionic tantalum oxide nanoparticle X-ray contrast agent, *ACS Nano* 6 (8) (2012) 6650-6658, <https://doi.org/10.1021/nn300928g>
- [32] G. Mohandas, N. Oskolkov, M. T. McMahon, P. Walczak, M. Janowski, Porous tantalum and tantalum oxide nanoparticles for regenerative medicine, *Acta Neurobiol. Exp.* 74 (2) (2014) 188-196,
- [33] N. Wang, J. Y. H. Fuh, S. T. Dheen, A. S. Kumar, Functions and applications of metallic and metallic oxide nanoparticles in orthopedic implants and scaffolds, *J. Biomed. Mater. Res.* 109 (2) (2021) 160-179, <https://doi.org/10.1002/jbm.b.34688>
- [34] H. Zhu, X. Ji, H. Guan, L. Zhao, L. Zhao, C. Liu, C. Cai, W. Li, T. Tao, J. E. Reseland, H. J. Haugen, J. Xiao, Tantalum nanoparticles reinforced polyetheretherketone shows enhanced bone formation, *Mater. Sci. Eng. C* 101 (2019) 232-242, <https://doi.org/10.1016/j.msec.2019.03.091>
- [35] A. Liguori, A. Bigi, V. Colombo, M. L. Focarete, M. Gherardi, C. Gualandi, M. C. Oleari, S. Panzavolta, Atmospheric pressure non-equilibrium plasma as a green tool to crosslink gelatin nanofibers, *Sci. Rep.* 6 (38542) (2016) 1-11, <https://doi.org/10.1038/srep38542>
- [36] P. K. Smith, R. I. Krohn, G. T. Hermanson, A. K. Mallia, F. H. Gartner, M. D. Provenzano, E. K. Fujimoto, N. M. Goeke, B. J. Olson, D. C Klenk, Measurement of protein using bicinchoninic acid, *Anal. Biochem.* 150 (1)(1985) 76-85, [https://doi.org/10.1016/0003-2697\(85\)90442-7](https://doi.org/10.1016/0003-2697(85)90442-7)
- [37] A.M. Reed, D.K. Gilding, Biodegradable polymers for use in surgery—poly(glycolic)/poly(lactic acid) homo and copolymers: 2. In vitro degradation, *Polymer* 22 (4) (1981) 494-498, [https://doi.org/10.1016/0032-3861\(81\)90168-3](https://doi.org/10.1016/0032-3861(81)90168-3)

- [38] C. Gualandi, N. Bloise, N. Mauro, P. Ferruti, A. Manfredi, M. Sampaolesi, A. Liguori, R. Laurita, M. Gherardi, V. Colombo, L. Visai, M. L. Focarete, E. Ranucci, Poly-l-Lactic Acid Nanofiber–Polyamidoamine Hydrogel Composites: Preparation, Properties, and Preliminary Evaluation as Scaffolds for Human Pluripotent Stem Cell Culturing, *Macromol Biosci.* 16 (10) (2016) 1533-1544, <https://doi.org/10.1002/mabi.201600061>
- [39] N.Horandghadim, J. Khalil-Allafi, Characterization of hydroxyapatite-tantalum pentoxide nanocomposite coating applied by electrophoretic deposition on Nitinol superelastic alloy, *Ceramics International* 45 (2019) 10448–10460, <https://doi.org/10.1016/j.ceramint.2019.02.105>
- [40] N. Hu, W. Wang, L. Lei, H. Fan, Y. Tan, H. Yuan, Z. Mao, P. Müller-Buschbaum, Q. Zhong, A hydrogen evolution system based on hybrid nanogel films with capabilities of spontaneous moisture collection and high light harvesting, *Green Chemistry.* 23 (2021) 8969-8978, <https://doi.org/10.1039/D1GC03322K>
- [41] N. Hu, L. Lin, J. Tan, W. Wang, L. Lei, H. Fan, J. Wang, P. Müller-Buschbaum, Q. Zhong, Wearable Bracelet Monitoring the Solar Ultraviolet Radiation for Skin Health Based on Hybrid IPN Hydrogels, *ACS Appl. Mater. Interfaces* 12 (2020) 56480-56490, <https://doi.org/10.1021/acsami.0c17628>
- [42] M. Nikkhah, F. Edalat, S. Manoucheri, A. Khademhosseini, Engineering microscale topographies to control the cell–substrate interface, *Biomaterials* 33 (21) (2012) 5230-5246, <https://doi.org/10.1016/j.biomaterials.2012.03.079>
- [43] R. A. Gittens, T. McLachlan, R. Olivares-Navarrete, Y. Cai, S. Berner, R. Tannenbaum, Z. Schwartz, K. H. Sandhage, B. D. Boyan, The effects of combined micron-/submicron-scale surface roughness and nanoscale features on cell proliferation and differentiation, *Biomaterials* 32 (13) (2011) 3395-3403, <https://doi.org/10.1016/j.biomaterials.2011.01.029>

- [44] A. B. Faia-Torres, M. Charnley, T. Goren, S. Guimond-Lischer, M. Rottmar, K. Maniura-Weber, N. D. Spencer, R. L. Reis, M. Textor, N. M. Neves, Osteogenic differentiation of human mesenchymal stem cells in the absence of osteogenic supplements: A surface-roughness gradient study, *Acta Biomater* 28 (2015) 64-75, <https://doi.org/10.1016/j.actbio.2015.09.028>
- [45] S. Khorshidi, A. Karkhaneh, Hydrogel/fiber conductive scaffold for bone tissue engineering, *J Biomed Mater Res A*. 106 (3) (2018) 718-724, <https://doi.org/10.1002/jbm.a.36282>